Virology 427 (2012) 18–24

Contents lists available at SciVerse ScienceDirect

Virology

journal homepage: www.elsevier.com/locate/yviro

Point mutations in the *West Nile virus (Flaviviridae; Flavivirus)* RNA-dependent RNA polymerase alter viral fitness in a host-dependent manner *in vitro* and *in vivo*

Greta A. Van Slyke [a], Alexander T. Ciota [a], Graham G. Willsey [a], Joachim Jaeger [b,c], Pei-Yong Shi [d], Laura D. Kramer [a,c,*]

[a] *The Arbovirus Laboratories, Wadsworth Center, New York State Dept. of Health, NY 12159, USA*
[b] *Department of Genetics, Wadsworth Center, New York State Dept. of Health, NY 12208, USA*
[c] *School of Public Health, State University of New York, NY 12205, USA*
[d] *Novartis Institute for Tropical Disease Pte Ltd., Singapore 138670, Singapore*

ARTICLE INFO

Article history:
Received 23 December 2011
Returned to author for revision
14 January 2012
Accepted 28 January 2012
Available online 23 February 2012

Keywords:
RNA viruses
Arbovirus
Flavivirus
Mutagenesis
RNA replication

ABSTRACT

The *West Nile virus* (WNV) genome contains a single RNA-dependent RNA polymerase (RdRp) gene, which is responsible for replication of the viral genome and, as such, is an important target for antiviral therapy. Viral RdRps are known to lack proofreading capabilities and as a result viruses such as WNV exist as a mixture of viral genotypes within an infection, enabling the virus to readily emerge and adapt to new host environments. To test the consequences of subtle structural alterations remote from the RdRp active-site, the following single point mutations were engineered in the WNV NS5 RdRp coding region: T363N, A365N, and T537I; these mutations were selected in an effort to stabilize the secondary structural elements near the rNTP binding pocket of the RdRp. Mutant viruses were tested *in vitro* on Vero, C6/36, *Culex tarsalis* and DF-1 cell types and *in vivo* in one day old chickens and *Culex pipiens* mosquitoes. Plaque morphology was affected by each mutation and growth and RNA replication kinetics were altered as well. Our results demonstrate that subtle alteration of the RdRp protein away from the active site can have a significant overall biological effect on WNV fitness, and that this effect can be host-dependent.

Introduction

West Nile virus (WNV; *Flaviviridae*; *Flavivirus*) was introduced into the United States more than a decade ago and now persists in local transmission cycles throughout North America (Kramer et al., 2007; Lanciotti et al., 1999). Unlike other flaviviruses (*i.e., St. Louis encephalitis virus*) which tend to cause geographically limited outbreaks, WNV has proven to be a generalist in terms of viral fitness, with the capacity to infect and replicate in a broad array of arthropod and avian hosts. This generalist nature has permitted the emergence and rapid dissemination of WNV in diverse ecological niches. All flaviviruses, including WNV, contain a single-strand positive-sense RNA genome, encoding a single polyprotein consisting of both structural (C, prM and E) and non-structural (NS1, 2a–b, 3, 4a–b and 5) proteins. The WNV NS5 is a bi-functional enzyme, with the N-terminal region consisting of the viral methyltransferase responsible for type-1 RNA cap formation and the C-terminal domain encoding the viral RNA-dependent RNA polymerase (RdRp) responsible for the *de novo* synthesis of the viral genome (Nomaguchi et al., 2004; Zhang et al., 2008). Viral RdRps have the highest error rate (lowest fidelity) of all known RNA polymerases with 0.1 to 1 nucleotide mutation per 10,000 bases copied (Domingo and Holland, 1994) or about 1 mutation per genome copied for WNV, with a genome length of just over 11 kilobases (kb). We have shown that WNV exists as a mutant spectrum within natural vectors and hosts and that mutant spectrum breadth plays an important role in viral pathogenesis, fitness, and adaptability (Ciota et al., 2007a, 2007b; Fitzpatrick et al., 2010; Jerzak et al., 2005, 2007). The low-fidelity viral RdRp acting in concert with a rapid viral replication cycle is most directly responsible for the mutant spectrum phenomenon commonly seen in flavivirus infections.

The crystal structure of the WNV RdRp resembles the classic viral RdRp architecture with thumb, palm and fingers sub-domains. Overall, the WNV RdRp structure displays many unique features when compared to both other flavivirus RdRps and more distantly related RdRps (Malet et al., 2007). To date there have been published studies to determine the basic mechanistic functions and molecular interactions of WNV RdRp indicating that the polymerase domain is a prime target for anti-viral drug development (Dong et al., 2008; Malet et al., 2008; Nomaguchi et al., 2004; Zhang et al., 2008). However, the consequence of altered polymerase function on mutant spectrum breadth, and subsequently viral adaptation, evolution, and pathogenesis has

* Corresponding author at: Wadsworth Center, NYSDOH Arbovirus Laboratory, 5668 State Farm Rd, Slingerlands, NY 12159, USA. Fax: +1 518 485 6669.
E-mail address: ldk02@health.state.ny.us (L.D. Kramer).

0042-6822/$ – see front matter © 2012 Elsevier Inc. All rights reserved.
doi:10.1016/j.virol.2012.01.036

yet to be determined for arthropod-borne (arbo) viruses. Specifically, the role of the RdRp in arboviral fitness and transmission in the mosquito and vertebrate hosts required for arbovirus maintenance is only starting to be examined. A recent study with Chikungunya virus (family *Togaviridae*; genus *Alphavirus*) examined the effects of arboviral RdRp mutation; where a single amino acid change that conferred mutagen resistance *in vitro* also lowered the fitness of the virus in its vector *Aedes aegypti* (Coffey et al., 2011). Our objective in this study was to begin to determine the role of the flavivirus RdRp in viral fitness (*i.e.*, the virus's ability to infect and replicate in a given host system) by subtle alteration of the WNV NS5 structure below the RdRp active site. We used computer modeling to determine where to incorporate amino acid substitutions, with the following residue changes engineered: NS5-T363N, NS5-A365N and NS5-T537I. Modeling indicates that none of these residues is in direct contact with the incoming rNTP, but instead they are positioned to stabilize residues below the rNTP binding pocket around amino acids NS5-D541 and NS5-D668 via hydrogen-bonding or van der Waals interactions (Figs. 1a–d). To determine WNV RdRp-mutant fitness, each virus was inoculated into various *in vitro* and *in vivo* host systems. Mutants were found to possess their own unique phenotype; all were attenuated when compared to the parental WNV strain *in vitro* and significant host-dependent attenuation was observed *in vivo* in one day old chicks and *Culex pipiens* mosquitoes. Therefore, we determined that subtle alteration of the WNV RdRp structure can have significant biological consequences with regard to viral fitness, and these consequences were found to be host-dependent, suggesting a host-specific mechanism involving the function of the viral RdRp.

Results

Rationale for introduced mutations

There is currently a lack of knowledge regarding the relationship between RdRp structure/function and viral fitness in natural hosts. Specifically, the role the RdRp plays in viral fitness and transmissibility in both vertebrate hosts and mosquito vectors of arboviruses is just beginning to be explored. We sought to modify the region near motif A in the WNV RdRp by introducing single amino acid changes in an effort to strengthen interactions and remotely stabilize the active site. Generally, the amino acid substitutions are conservative, but possess slightly longer side chains, and, therefore, a local strengthening of hydrogen bond and van der Waals interactions is predicted. Residues 363 and 365 have been mutated to asparagine, whereby the longer, polar side chain is poised to interact with carbonyl oxygen and backbone nitrogen atoms in a helical turn within RdRp motif A (residues 541–546) (Figs. 1b and c). Thr537 has been mutated to isoleucine in an attempt to strengthen van der Waals interactions with a neighboring Trp540 (Fig. 1d). Thus, the strengthening of side-chain/side-chain interactions near RdRp motifs A and C is thought to result in an overall stabilization of the WNV RdRp active site.

Assessment of plaque morphology

Upon initial titration of the RdRp mutant viruses, significant reduction of plaque size was observed [$p<0.01$ for all mutants compared to WNV- infectious clone (IC)]; where mean plaque diameters were

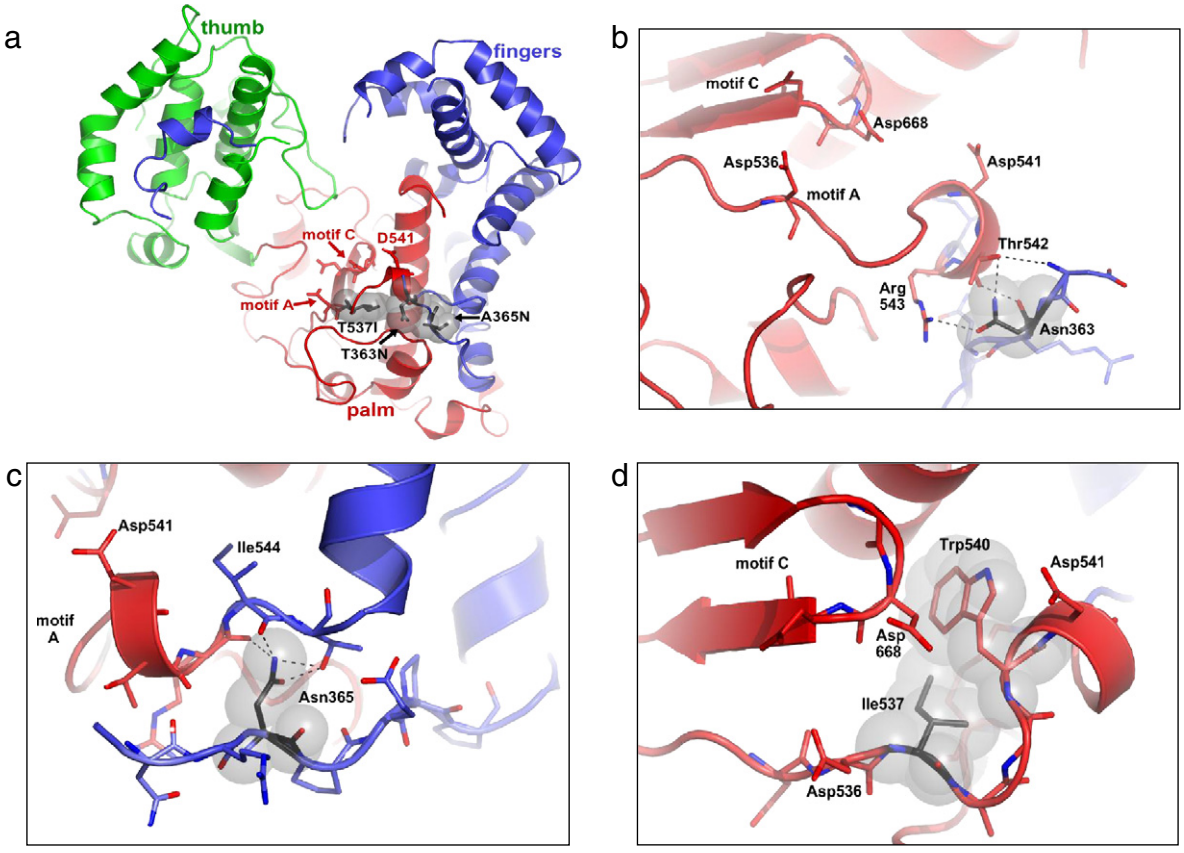

Fig. 1. The overall structure of WNV NS5 RdRp colored according to the polymerase sub-domains (a). The RdRp active site is indicated as motifs A and C (black arrows). Detail of the side chain interactions of residues Asn363 (b), Asn365 (c) and Ile537 (d) with the remainder of the WNV RdRp active site. Note that mutations are not directly located in the RdRp active site but structurally support the loop containing motif A. Most of the polar (dashed lines) or van der Waals (gray spheres) interactions are designed to stabilize a short helical turn in RdRp motif A, which is involved in binding of magnesium ions and the incoming rNTPs. This figure was generated in PyMol using PDB entries 2HCN and 2HFZ as starting coordinates (Malet et al., 2008).

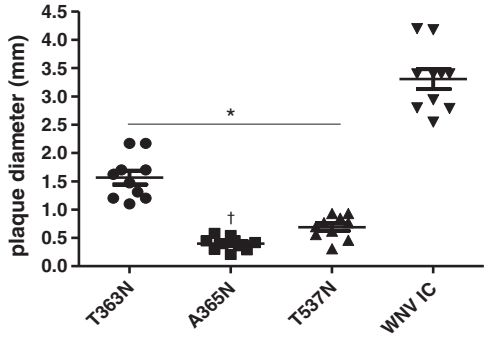

Fig. 2. Mutant plaque size reduction as compared to parental WNV-IC. Significance for all mutants as compared to WNV-IC ($p<10^{-6}$) denoted with (*). Significance for A365N as compared to T363N and T537I ($p<0.004$) denoted with (†).

3.3, 1.56, 0.7 and 0.4 mm for WNV-IC, T363N, T537I and A365N respectively (Fig. 2).

NS5 mutant growth kinetics in vitro

In an effort to characterize growth kinetics in a variety of hosts *in vitro*, primary stocks of RdRp mutant viruses along with the WNV-IC were inoculated on four cell types: Vero (mammalian), C6/36 (*Aedes albopictus*), CxT (*Culex tarsalis*), and DF-1 (avian) (Fig. 3), following infection at a multiplicity of infection (MOI) of 0.01. Statistical comparisons of growth kinetics of mutant viruses and WNV-IC by *t*-test were completed at all time points. NS5 mutant viruses demonstrated varying degrees of attenuation in all cell types tested (Fig. 3). In Vero cells (Fig. 3a), NS5-T363N and T537I viruses grew to significantly lower titers ($p<0.01$) at 24 h post-inoculation (p.i.) and A365N ($p<0.01$) grew to significantly lower titers at all time-points tested when compared to the WNV-IC. In C6/36 cells (Fig. 3b), all mutant viruses, compared to the WNV-IC, grew to significantly lower titers at 48 h p.i. and NS5-T537I was significantly attenuated ($p<0.05$) at 24 and 48 h p.i. Again, NS5-A365N was significantly ($p<0.01$) attenuated at all time-points tested when compared to WNV-IC growth kinetics. Similar results were obtained for growth on CxT cells (Fig. 3c), where all mutant viruses grew to significantly lower titers at 48 h p.i. ($p<0.02$ for T363N and T537I; $p<0.01$ for A365N). Mutant NS5-T537I also grew to significantly lower titers at 72 h and 96 h ($p<0.01$) p.i.; and NS5-T363N was also attenuated at 72 h p.i. The growth of NS5-A365N virus was significantly attenuated ($p<0.01$) on CxT cells at 24 h, 48 h and 96 h post-inoculation. The most dramatic levels of attenuated growth kinetics for NS5 mutant viruses were seen in the avian DF-1 cell line (Fig. 3d), where all NS5 mutant viral growth was significantly attenuated at all time-points sampled with the NS5-A365N mutant again displaying the most attenuated growth phenotype.

RNA replication kinetics in vitro

In order to determine if RNA replication, was compromised as a result of the engineered mutations; C6/36 cells were infected at a MOI of 10 with primary stocks of WNV RdRp mutants and WNV-IC, viron production in the supernatant was measured by plaque assay at 8, 12 and 24 h p.i. and RNA copy numbers were determined for each time-point by quantitative RT-PCR. The results at 24 h p.i. (Fig. 4) show all WNV-NS5 mutant viruses are significantly deficient in RNA replication when compared to the WNV-IC ($p<0.05$ for T363N and T537I and $p<0.01$for A365N), in particular WNV-NS5

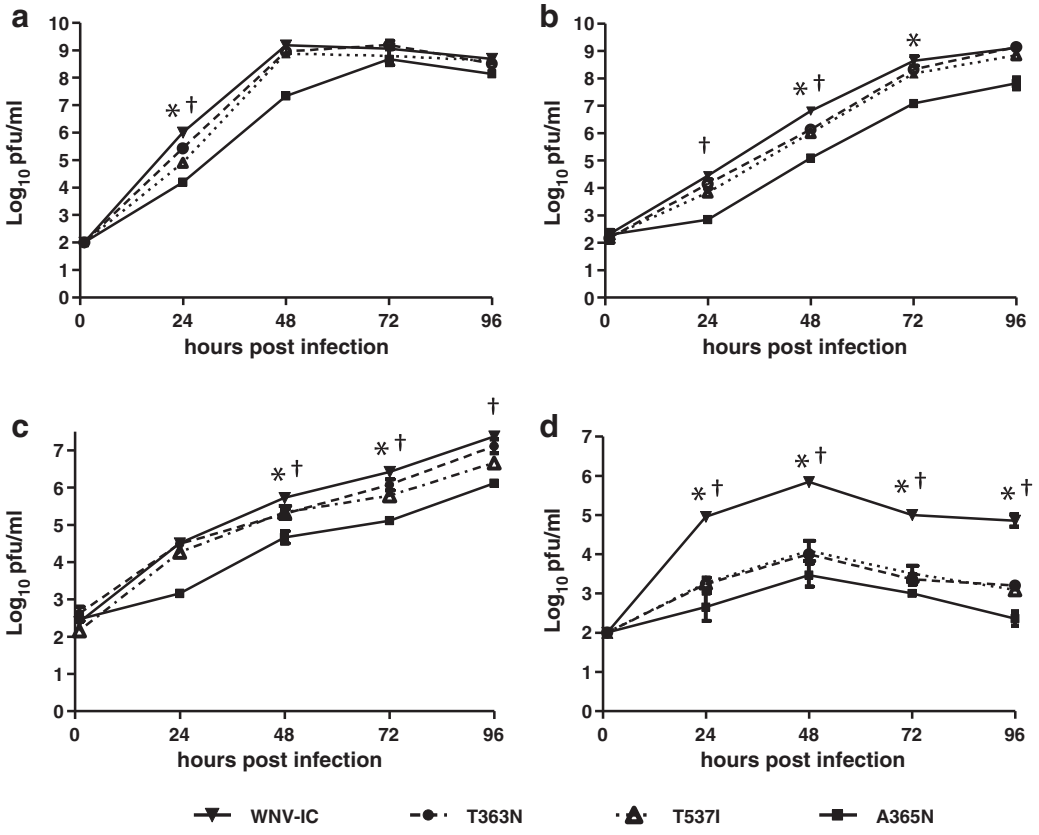

Fig. 3. NS5 mutant growth kinetics *in vitro* in Vero (a), C6/36 (b), *C. tarsalis* (c) and DF-1 (d) cell lines. Data points represent the mean titer of triplicate well infection at MOI 0.01. Viral titers of NS5 A365N are significantly lower than WNV-IC at all time points in all cell lines (*t*-test, $p<0.05$). Significant differences in viral titers for NS5 T363N and T537I relative to WNV-IC are denoted by * and †, respectively.

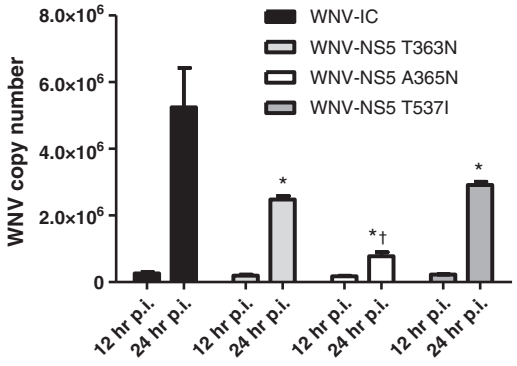

Fig. 4. WNV RNA replication on C6/36 cell culture. Confluent monolayers of C6/36 cells were infected at a M.O.I. of 10; supernatant was harvested and RNA extracted at 12 and 24 h post-infection. Real-time RT-PCR was performed to determine viral RNA copy numbers. Significant differences relative to WNV-IC (T363N $p<0.02$, A365N $p<0.001$ and T537I $p<0.03$) denoted with (*). Significant differences relative to T363N ($p<0.001$) and T537I ($p<0.0005$) denoted with (†).

A365N was significantly deficient in RNA replication not only when compared to WNV-IC but also when compared to both WNV-NS5 T363N and T537I ($p<0.01$). Results for 8 and 12 h p.i. with respect to RNA copy number were indistinguishable, therefore only the 12 h p.i. time-point is represented in Fig. 4. Copy number data correlated with infectious particles (pfu) detected (data not shown) for these samples, where each mutant displayed a significant titer reduction ($p<0.01$) at 24 h p.i., when compared to WNV-IC, relative to its deficiency in RNA replication.

NS5 mutant growth kinetics in vivo

Viral growth kinetics *in vitro* do not always correlate with the kinetics within host organisms. Therefore we conducted viremia studies in one day-old chickens and evaluated viral growth in *C. pipiens* mosquitoes. One day old chickens were inoculated with 100 pfu of virus sub-cutaneously in the neck and five chicks per virus were bled by the brachial vein every 24 h for up to 120 h post-inoculation (p.i.). Viral titers were determined by plaque assay on Vero cells. Replicative fitness of WNV-NS5 mutants *in vivo* in chickens and mosquitoes was found to be host-dependent (Fig. 5). Varying degrees of attenuation of viremia in one day-old chickens of all NS5 mutant viruses was observed compared to the WNV-IC (Fig. 5a). At one day p.i. viremia was attenuated for all mutants. At day 2 p.i., peak viremia for WNV-IC, all mutant viruses were significantly attenuated ($p<0.01$); at day 3 p.i. both NS5-T363N and A365N were significantly attenuated. The largest difference in serum titers among NS5 mutants was seen at day 2 p.i., where NS5-A365N was significantly attenuated compared to both T363N and T537I. Consensus sequencing of the NS5 region of RNA extracted from day 5 p.i. chick serum confirmed that there was no detectable reversion of mutant viruses.

Viral growth was measured in *C. pipiens* mosquitoes (Fig. 5b), an important urban vector of WNV, by way of intrathoracic (IT) inoculation of 10 pfu of virus and sampling at days 1–5, 8, 14, and 21 p.i. Surprisingly, none of the mutant viruses differed significantly in growth kinetics when compared to the WNV-IC or each other. These results are in contrast to what was seen *in vitro* in both mosquito cell types (C6/36 and CxT) where all NS5 mutant viruses displayed varying degrees of attenuation. Consensus sequencing of the NS5 region of RNA extracted from day 21 p.i. mosquito homogenate confirmed no detectable reversion of mutant viruses.

Discussion

The arboviral RdRp is responsible for the replication of the viral genome and the generation of the mutant spectrum, which has

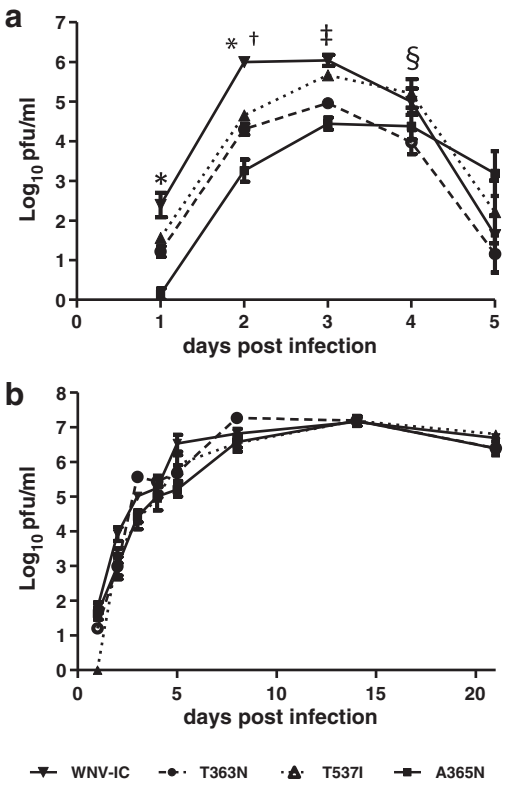

Fig. 5. WNV *in vivo* growth kinetics in day-old chickens (a) data points represent mean serum titer of five chicks inoculated SC with 100 pfu virus, significant difference relative to WNV-IC for all mutants denoted with (*) ($p<0.03$), significant difference of A365N relative to T363N and T537I denoted with (†), significant difference of both A365N and T363N relative to WNV-IC ($p<0.0003$) denoted with (‡), and significant difference of A365N relative to WNV-IC denoted with (§). Viral growth kinetics in *C. pipiens* mosquitoes (b). Data points represent mean titer of five mosquitoes inoculated IT with 10 pfu virus.

proven to be important in arboviral fitness, adaptability and pathogenesis in a host-dependent manner (Ciota et al., 2007a, 2007b; Fitzpatrick et al., 2010; Jerzak et al., 2005, 2007). The flavivirus RdRp is considered a prime target for new antiviral drug therapy, as the mammalian hosts of these viruses do not possess such a polymerase (Cerutti, 2006); however, the specific mechanisms governing the role of the RdRp in viral fitness, transmission, pathogenesis and host adaptation have only begun to be explored. In order to evaluate the consequence of altered polymerase structure on the infectivity, growth and replication of WNV in relevant hosts we constructed three NS5-RdRp mutant WNV strains: NS5-T363N, A365N and T537I each possessing a structurally plausible single amino acid change, some 15 Å away from the conserved aspartates in the RdRp active site. Initially significant reductions in plaque size were noted for all mutant viruses, in particular mutant NS5-A365N (Fig. 2). *In vitro* assessment of growth kinetics in relevant host-type cell lines demonstrated significant attenuation of varying degrees for all mutant viruses, again particularly with NS5-A365N (Fig. 3).

In day-old chickens, viremia of NS5 mutants correlated with results in cell culture growth assays, particularly DF-1 cells, where all mutants are significantly attenuated, NS5-A365N most significantly. Typically peak WNV viremia titers are seen at day 2 p.i. in chicks, yet for all NS5 mutants peak titers were not reached until 3 to 4 days p.i. and no mutant reached the same peak titer as the parental virus, WNV-IC (Fig. 5a). These results are consistent with a significant decrease in viral fitness for mutant viruses, due to the structural changes introduced by our point mutations.

To assess the impact of the point mutations on viral RNA replication, quantitative RT-PCR assays were performed on supernatant collected

from infected C6/36 cell cultures 12 h and 24 h p.i (Fig. 3). The results demonstrate that all mutant viruses are significantly deficient in RNA replication when compared to WNV-IC at 24 h, and mutant A365N is most significantly deficient. The number of infectious particles for each virus at 12 and 24 h p.i. directly correlates with the magnitude of RNA replication deficiency, indicating a defect in RNA replication brought about by the engineered point mutations as the cause of the significantly attenuated growth characteristics of these mutant viruses both *in vitro* and in day-old chickens. Confounding this conclusion is the finding that all mutant viruses, particularly A365N, were equally able to infect and replicate in a natural mosquito vector, *C. pipiens*, in contrast to *in vitro* growth kinetics on two mosquito cell lines (Figs. 3a and b) where significant attenuation was observed for mutant A365N at 24, 48, 72 and 96 h p.i. This result highlights the importance of validating data obtained through cell culture assay *in vivo* in natural hosts. Moreover, when compared to viremia kinetics in day-old chickens, this result is indicative of a host-specific mechanism at the level of the RdRp as a determinant of successful viral infection and replication.

Single point mutations of the viral RdRp have previously been shown to confer substantial biological consequences; a single point mutation in PV 3Dpol (G64S) significantly decreased viral pathogenicity and constrained mutant swarm composition by increasing RdRp fidelity (Pfeiffer and Kirkegaard, 2005; Vignuzzi et al., 2006, 2008). Inspection of various (complete) PV 3Dpol and related picornavirus RdRp structures and experimental data suggests that this mutation near RdRp motif A changes local interactions and can modify the stability and kinetics of the active site (Arnold et al., 2005). A single amino acid mutation in the foot-and-mouth disease virus (*Picornaviridae*; *Aphthovirus*) polymerase catalytic site was found to confer resistance to the nucleoside analog ribavirin without consequence to viral growth or polymerase fidelity (Arias et al., 2008; Sierra et al., 2007). However, the consequence of such mutations on the flavivirus RdRp has not been examined. The loop that harbors the mutations we inserted near motif A of the WNV NS5 is located on the surface of the RdRp domain near the fingers/palm sub-domain junction. Surface-exposed loops are found in similar positions in flavivirus, picornavirus and other related RdRp structures (Malet et al., 2008). We suspect that this region could not only be involved in stabilizing residues in the polymerase active site, but could also serve as a module that interacts with other replicase components (MTase, helicase *etc.*) and possibly even host-factor proteins. Positions NS5-363 and 365 are located in the fingers subdomain and are within a signature region shown for DENV to be a functional nuclear localization sequence known as “bNLS” (Brooks et al., 2002; Forwood et al., 1999). DENV NS5 has been shown to localize to the nucleus of infected cells, however, WNV NS5 is not known to localize to the nucleus (Malet et al., 2008). The bNLS region of DENV-2 has also been shown to directly interact with the c-terminus of the helicase (NS3) component of the replicase complex (Johansson et al., 2001), the structures of the WNV and DENV bNLS region within the RdRp are nearly identical (Malet et al., 2008), therefore, a putative mechanism for the deficiencies displayed for mutants T363N and A365N could be a disruption of optimal interactions of the replicase complex. Further biochemical studies are needed to confirm this mechanism. In addition, the Thr residue at position 363 has been conserved across all flaviviruses sequenced thus far (Davidson, 2009) and our results suggest that even a conservative change at this position can have a significant negative biological effect at the level of RNA replication.

Elements within the bNLS/Motif A region of the RdRp are thought to play an important role in overall pol structure (Davidson, 2009; Malet et al., 2008) and the most dramatic structural change to the RdRp was predicted to be mutant A365N; as a result this mutant displayed severe and significant phenotypic effects on cell culture and in chickens. More interesting is that this attenuation did not carry over *in vivo* to the mosquito vector *C. pipiens*, despite having significant deficiencies in RNA replication and growth in *A. albopictus* and *C. tarsalis* mosquito cell lines. A possible explanation for this could be a host-specific interaction between the viral RdRp/replicase complex and vector cell machinery which allows the virus to function optimally despite a sub-optimal structure. Involvement of host-factors in this particular region of the WNV RdRp could explain the host-dependent effects seen in this study. Thus far studies have shown that the recruitment of host proteases in both the insect and vertebrate is required for viral polyprotein processing and a recent study demonstrated at least 18 mosquito proteins can interact with the WNV and DENV envelope, capsid, NS2a, and NS4b viral proteins in mosquito cell culture (Colpitts et al., 2011). However, little is known about host-factors that may interact with the viral replicase complex.

Our results represent an important investigation of the role of WNV RdRp structure in the growth kinetics and RNA replication of an arbovirus and demonstrate that subtle, single point mutations in the flavivirus RdRp can have profound phenotypic consequences. Future studies will help elucidate the specific mechanisms of attenuation and host protein interactions which may be enhancing viral replication in the mosquito vector and also determine how these consequences might relate to mutant swarm composition.

Materials and methods

Viruses

The *West Nile virus* infectious clone (WNV-IC) virus was generated from an infectious cDNA clone based on WNV strain 3356 (AF404756). Methods for clone manipulation and rescue of infectious WNV are as described previously (Shi et al., 2002). Using PyMOL, mutant WNV NS5-T363N, A365N, T537I were designed by close inspection of the WNV RdRp crystal structure (Fig. 1) superimposed with other structurally related and appropriately aligned RdRps from *Dengue virus* (DENV), *Foot and mouth disease virus* (FMDV) and *Poliovirus* (PV). The mutants shown in Table 1 were generated by site-directed mutagenesis (SDM) of the WNV-IC using the QuikChange XLII SDM kit (Stratagene, La Jolla, CA) as per the manufacturer's protocol. Mutant WNV-IC DNA was then amplified in *E. coli* and plasmid harvested by Highspeed Midiprep (Qiagen, Valencia, CA). Full genome sequencing of NS5 mutant WNV-IC plasmids indicated no other mutations were present except those engineered.

All mutant and control WNV-IC plasmids were transcribed using the MEGAscript kit (Ambion, Austin, TX) and assembled as per manufacturer's protocol. Resulting RNA was purified with the MEGAclear kit (Ambion). Wild-type WNV-IC RNA and mutant RNAs: WNV-NS5 T363N, NS5 A365N, NS5 T537I, were electroporated into C6/36 cells using a GenePulser (BioRad, Hercules, CA). Supernatants were collected from days 3 to 7 post-transfection; these primary viral stocks were used as inocula for all viral growth experiments. WNV infectious particles were quantified by plaque assay on Vero cells.

In order to determine the stability of the engineered mutations all mutant viruses were subjected to an independent blind passage series and sequenced after 3 blind passages in C6/36 cells, no reversions were detected. Passaged viruses were not used in any of the viral growth studies described herein.

Table 1
WNV NS5 mutations.

Amino acid change[a]	Codon position[a]	Codon change
T363N	1087–9	ACG → A**AC**
A365N	1093–5	GCT → **AA**T
T537I	1609–11	ACA → A**TC**

[a] Position number for amino acid and nucleotide codons based on NS5 sequence.

Cell culture

African green monkey kidney cells (Vero, ATCC #CCL-81); *A. albopictus* mosquito cells (C6/36, ATCC #CRL-1660); Chicken embryo fibroblast cells (DF-1, ATCC #CRL-12203); and *C. tarsalis* (CxT) cells, originally from UC Davis and kindly provided by A. Brault were used for *in vitro* viral growth assays.

Experimental hosts

Specific pathogen free (SPF) chicken eggs (*Gallus gallus*) were obtained from Sunrise Farms (Catskill, NY) and hatched in a brooder incubator (G.Q.C. Brand, GA) at the Arbovirus Laboratory. Colonized *C. pipiens* mosquitoes were originally derived from larvae collected in Pennsylvania and maintained at the Wadsworth Center Arbovirus Laboratories since 2004. Rearing procedures and conditions for experimental mosquitoes are described elsewhere (Ebel et al., 2004).

Plaque size determination and in vitro growth kinetics

Plaque phenotype of primary virus stocks of WNV-IC and NS5 mutant viruses was determined by plaque assay on Vero cells. At least 10 plaques per strain were measured using Zeiss Axioscope software. Statistical comparisons of plaque size differences were done by paired *t*-test analysis.

Viral growth kinetics were determined using confluent Vero, C6/36, CxT and DF-1 cell monolayers in 6-well plates following inoculation with a multiplicity of infection (MOI) of 0.01 of each primary virus stock in triplicate. After 1 h of incubation inoculum was removed and monolayers were washed and overlaid with 3 ml of maintenance media. Supernatant samples were taken at 24, 48, 72 and 96 h post-inoculation and titrated on Vero cells in duplicate by plaque assay. Growth curves were plotted using mean titer per time-point.

For one step growth kinetic analysis, C6/36 cell monolayers in 6-well plates were inoculated with a MOI of 10 in triplicate for each mutant virus and WNV-IC primary virus stock. Absorption of the virus was allowed for 1 h at 28 °C, then wells were washed and overlaid with media; supernatant samples were taken at 8, 12, and 24 h post-inoculation. Samples were titrated on Vero cells in duplicate by plaque assay; RNA was extracted from all supernatants using the QiAmp viral RNA spin columns (Qiagen) and used for RNA copy number analysis by TaqMan (Applied Biosystems, Carlsbad, CA) using a primer/probe set specific to the WNV E gene (Shi et al., 2001); reactions were set up as per the manufacturer's protocol. Comparative differences in copy number were analyzed by *t*-test using geometric mean values.

Viremia kinetics in chickens

One day old SPF chickens in groups of 5 were infected by subcutaneous inoculation with 100 pfu of primary stock virus in 0.1 ml animal inoculation diluent (endotoxin free phosphate-buffered saline supplemented with 1% FBS) per group, along with 2 mock inoculated chickens (diluent only). All groups were housed separately in adjacent cages. Chickens were bled from the brachial vein at days 1 through 4 post-inoculation and 50 μl of blood was collected via capillary action into serum separator tubes, separated, aliquoted, and used to determine the infectious WNV titer by plaque assay on Vero cells. On day 5 post-inoculation, chicks were given a lethal dose of Sleepaway (Fort Dodge Animal Health, Fort Dodge, IA) and cardiac puncture was performed to collect blood. Serum was used to determine the infectious WNV titer by plaque assay on Vero cells and to extract viral RNA using Qiamp viral RNA spin columns (Qiagen) for subsequent sequence verification.

Viral growth kinetics in mosquitoes

Fifty female *C. pipiens* mosquitoes per virus were infected by intrathoracic inoculation with 10 pfu primary virus stock each. Mosquitoes were held for 21 days at 27 °C and maintained on a 10% sucrose solution. Five mosquitoes were harvested on days 1 through 5, 7, 14, and 21 post-inoculation for each virus. Bodies were homogenized and mosquito debris was removed by centrifugation, the resulting supernatant was used for titration by plaque assay on Vero cells. An aliquot of day 21 homogenate was taken for RNA extraction with Qiamp viral RNA kit (Qiagen) and used for subsequent sequence verification.

NS5 Sequencing

In order to dismiss the possibility of reversion, all mutant viruses were subjected to NS5 sequencing after *in vitro* and *in vivo* analysis. RNA extracted from day 5 chick serum, day 21 mosquito harvest, day 4 cell culture supernatant were subjected to reverse transcription (RT) and polymerase chain reactions (PCR) using the Qiagen One-Step RT-PCR kit (Qiagen) with 3 primer sets encompassing the NS5 RdRp region (sequences available upon request). All sequencing was carried out at the Wadsworth Center Applied Genomics Technology Core (WCAGTC) on an ABI 3100 or 3700 automated sequencer (Applied Biosystems).

Full genome consensus sequencing

To verify the presence of only the desired mutations, full genome sequencing was performed on primary virus stocks of all NS5 mutant WNV created by SDM, the full genome was amplified by RT-PCR in 10 overlapping fragments using one-step RT-PCR (Qiagen). A complete list of amplification and sequencing primers is available from the author upon request. Consensus sequencing was performed as previously described (Davis et al., 2005).

Sequence analysis

Sequences were compiled and edited using the SeqMan module of the DNAStar software package (DNAStar, Inc., Madison, WI) and a minimum of two-fold redundancy throughout each clone or consensus fragment was required for sequence data to be considered complete.

Molecular modeling

Polymerase crystal structures of WNV, DENV, *Poliovirus* and *Foot-and-mouth disease virus* were superimposed using the program PyMOL (http://www.pymol.org) and backbone-dependent side chain rotamers in the Mutagenesis Wizard used to introduce mutations. Any steric clashes were removed through manual adjustments followed by energy minimization implemented in the program NAMD2 (http://www.ks.uiuc.edu/Research/namd).

Acknowledgments

This work was supported by NIH grant AI077669. The authors would like to thank the Wadsworth Center Applied Genomics Technology core for sequencing, Tissue Culture Core facility for providing cells and media and the Wadsworth Center Veterinary Services. We would also like to thank Rachael Viscio, Jean Demarco, Pamela Chin and David Young for their technical assistance in this study.

References

Arias, A., Arnold, J.J., Sierra, M., Smidansky, E.D., Domingo, E., Cameron, C.E., 2008. Determinants of RNA-dependent rna polymerase (in)fidelity revealed by kinetic analysis of the polymerase encoded by a foot-and-mouth disease virus mutant with reduced sensitivity to ribavirin. J. Virol. 82, 12346–12355.

Arnold, J.J., Vignuzzi, M., Stone, J.K., Andino, R., Cameron, C.E., 2005. Remote site control of an active site fidelity checkpoint in a viral RNA-dependent RNA polymerase. J. Biol. Chem. 280, 25706–25716.

Brooks, A.J., Johansson, M., John, A.V., Xu, Y., Jans, D.A., Vasudevan, S.G., 2002. The interdomain region of dengue NS5 protein that binds to the viral helicase NS3 contains independently functional importin beta 1 and importin alpha/beta-recognized nuclear localization signals. J. Biol. Chem. 277, 36399–36407.

Cerutti, H.C.-M.J.A., 2006. On the origin and functions of RNA-mediated silencing: from protists to man. Curr. Genet. 50, 81–99 (Ref Type: Generic).

Ciota, A.T., Lovelace, A.O., Jones, S.A., Payne, A., Kramer, L.D., 2007a. Adaptation of two flaviviruses results in differences in genetic heterogeneity and virus adaptability. J. Gen. Virol. 88, 2398–2406.

Ciota, A.T., Lovelace, A.O., Ngo, K.A., Le, A.N., Maffei, J.G., Franke, M.A., Payne, A.F., Jones, S.A., Kauffman, E.B., Kramer, L.D., 2007b. Cell-specific adaptation of two flaviviruses following serial passage in mosquito cell culture. Virology 357, 165–174.

Coffey, L.L., Beeharry, Y., Borderia, A.V., Blanc, H., Vignuzzi, M., 2011. Arbovirus high fidelity variant loses fitness in mosquitoes and mice. Proc. Natl. Acad. Sci. U. S. A. 108, 16038–16043.

Colpitts, T.M., Cox, J., Nguyen, A., Feitosa, F., Krishnan, M.N., Fikrig, E., 2011. Use of a tandem affinity purification assay to detect interactions between West Nile and dengue viral proteins and proteins of the mosquito vector. Virology 417, 179–187.

Davidson, A.D., 2009. Chapter 2. New insights into flavivirus nonstructural protein 5. Adv. Virus Res. 74, 41–101.

Davis, C.T., Ebel, G.D., Lanciotti, R.S., Brault, A.C., Guzman, H., Siirin, M., Lambert, A., Parsons, R.E., Beasley, D.W., Novak, R.J., Elizondo-Quiroga, D., Green, E.N., Young, D.S., Stark, L.M., Drebot, M.A., Artsob, H., Tesh, R.B., Kramer, L.D., Barrett, A.D., 2005. Phylogenetic analysis of North American West Nile virus isolates, 2001–2004: evidence for the emergence of a dominant genotype. Virology 342, 252–265.

Domingo, E., Holland, J.J., 1994. Mutation rates and rapid evolution of RNA viruses. In: Morse, S.S. (Ed.), Evolutionary Biology of Viruses. Raven Press, New York, pp. 161–184.

Dong, H., Zhang, B., Shi, P.Y., 2008. Terminal structures of West Nile virus genomic RNA and their interactions with viral NS5 protein. Virology 381, 123–135.

Ebel, G.D., Carricaburu, J., Young, D., Bernard, K.A., Kramer, L.D., 2004. Genetic and phenotypic variation of West Nile virus in New York, 2000–2003. Am.J.Trop. Med. Hyg. 71, 493–500.

Fitzpatrick, K.A., Deardorff, E.R., Pesko, K., Brackney, D.E., Zhang, B., Bedrick, E., Shi, P.Y., Ebel, G.D., 2010. Population variation of West Nile virus confers a host-specific fitness benefit in mosquitoes. Virology 404, 89–95.

Forwood, J.K., Brooks, A., Briggs, L.J., Xiao, C.Y., Jans, D.A., Vasudevan, S.G., 1999. The 37-amino-acid interdomain of dengue virus NS5 protein contains a functional NLS and inhibitory CK2 site. Biochem. Biophys. Res. Commun. 257, 731–737.

Jerzak, G., Bernard, K.A., Kramer, L.D., Ebel, G.D., 2005. Genetic variation in West Nile virus from naturally infected mosquitoes and birds suggests quasispecies structure and strong purifying selection. J. Gen. Virol. 86, 2175–2183.

Jerzak, G.V., Bernard, K., Kramer, L.D., Shi, P.Y., Ebel, G.D., 2007. The West Nile virus mutant spectrum is host-dependant and a determinant of mortality in mice. Virology 360, 469–476.

Johansson, M., Brooks, A.J., Jans, D.A., Vasudevan, S.G., 2001. A small region of the dengue virus-encoded RNA-dependent RNA polymerase, NS5, confers interaction with both the nuclear transport receptor importin-beta and the viral helicase, NS3. J. Gen. Virol. 82, 735–745.

Kramer, L.D., Styer, L.M., Ebel, G.D., 2007. A global perspective on the epidemiology of West Nile virus. Annu. Rev. Entomol. 53, 61–81.

Lanciotti, R.S., Roehrig, J.T., Deubel, V., Smith, J., Parker, M., Steele, K., Crise, B., Volpe, K.E., Crabtree, M.B., Scherret, J.H., Hall, R.A., MacKenzie, J.S., Cropp, C.B., Panigrahy, B., Ostlund, E., Schmitt, B., Malkinson, M., Banet, C., Weissman, J., Komar, N., Savage, H.M., Stone, W., McNamara, T., Gubler, D.J., 1999. Origin of the West Nile virus responsible for an outbreak of encephalitis in the northeastern United States. Science 286, 2333–2337.

Malet, H., Egloff, M.P., Selisko, B., Butcher, R.E., Wright, P.J., Roberts, M., Gruez, A., Sulzenbacher, G., Vonrhein, C., Bricogne, G., Mackenzie, J.M., Khromykh, A.A., Davidson, A.D., Canard, B., 2007. Crystal structure of the RNA polymerase domain of the West Nile virus non-structural protein 5. J. Biol. Chem. 282, 10678–10689.

Malet, H., Masse, N., Selisko, B., Romette, J.L., Alvarez, K., Guillemot, J.C., Tolou, H., Yap, T.L., Vasudevan, S.G., Lescar, J., Canard, B., 2008. The flavivirus polymerase as a target for drug discovery. Antivir. Res. 80, 23–35.

Nomaguchi, M., Teramoto, T., Yu, L., Markoff, L., Padmanabhan, R., 2004. Requirements for West Nile virus (−)- and (+)-strand subgenomic RNA synthesis in vitro by the viral RNA-dependent RNA polymerase expressed in *Escherichia coli*. J. Biol. Chem. 279, 12141–12151.

Pfeiffer, J.K., Kirkegaard, K., 2005. Increased fidelity reduces poliovirus fitness and virulence under selective pressure in mice. PLoS Pathog. 1, e11.

Shi, P.-Y., Kauffman, E.B., Ren, P., Felton, A., Tai, J.H., Dupuis II, A.P., Jones, S.A., Ngo, K.A., Nicholas, D.C., Maffei, J.G., Ebel, G.D., Bernard, K.A., Kramer, L.D., 2001. High throughput detection of West Nile virus RNA. J. Clin. Microbiol. 39, 1264–1271.

Shi, P.Y., Tilgner, M., Lo, M.K., Kent, K.A., Bernard, K.A., 2002. Infectious cDNA clone of the epidemic West Nile virus from New York City. J. Virol. 76, 5847–5856.

Sierra, M., Airaksinen, A., Gonzalez-Lopez, C., Agudo, R., Arias, A., Domingo, E., 2007. Foot-and-mouth disease virus mutant with decreased sensitivity to ribavirin: implications for error catastrophe. J. Virol. 81, 2012–2024.

Vignuzzi, M., Stone, J.K., Arnold, J.J., Cameron, C.E., Andino, R., 2006. Quasispecies diversity determines pathogenesis through cooperative interactions in a viral population. Nature 439, 344–348.

Vignuzzi, M., Wendt, E., Andino, R., 2008. Engineering attenuated virus vaccines by controlling replication fidelity. Nat. Med. 14, 154–161.

Zhang, B., Dong, H., Zhou, Y., Shi, P.Y., 2008. Genetic interactions among the West Nile virus methyltransferase, the RNA-dependent RNA polymerase, and the 5′ stem-loop of genomic RNA. J. Virol. 82, 7047–7058.